Wang *et al. Microbial Cell Factories* (2025) 24:105
https://doi.org/10.1186/s12934-025-02722-z

Microbial Cell Factories

RESEARCH Open Access

A highly efficient heterologous expression platform to facilitate the production of microbial natural products in *Streptomyces*

Xiuling Wang[1], Ping Lin[2], Qiyao Shen[1], Xueyan Feng[2], Shouying Xu[1], Qijun Zhang[1], Yang Liu[1], Cailing Ren[1], Daojing Yong[1], Qiong Duan[1], Liujie Huo[1], Youming Zhang[1], Gang Li[2*], Jun Fu[1*] and Ruijuan Li[1*]

Abstract

Background Heterologous expression in *Streptomyces* provides a platform for mining natural products (NPs) encoded by cryptic biosynthetic gene clusters (BGCs) of bacteria. The BGCs are first engineered in hosts with robust recombineering systems, such as *Escherichia coli*, followed by expression in optimized heterologous hosts, such as *Streptomyces*, with defined metabolic backgrounds.

Results We developed a highly efficient heterologous expression platform, named Micro-HEP (*micro*bial *h*eterologous *e*xpression *p*latform), that uses versatile *E. coli* strains capable of both modification and conjugation transfer of foreign BGCs and optimized chassis *Streptomyces* strain for expression. The stability of repeat sequences in these *E. coli* strains was superior to that of the commonly used conjugative transfer system *E. coli* ET12567 (pUZ8002). For optimizing expression of foreign BGCs, the chassis strain *S. coelicolor* A3(2)-2023 was generated by deleting four endogenous BGCs followed by introducing multiple recombinase-mediated cassette exchange (RMCE) sites in the *S. coelicolor* A3(2) chromosome. Additionally, modular RMCE cassettes (Cre-lox, Vika-vox, Dre-rox, and phiBT1-attP) were constructed for integrating BGCs into the chassis strain. Micro-HEP was tested using BGCs for the anti-fibrotic compound xiamenmycin and griseorhodins. Two to four copies of the *xim* BGC were integrated by RMCE, with increasing copy number associated with increasing yield of xiamenmycin. The *grh* BGC was also efficiently expressed, and the new compound griseorhodin H was identified.

Conclusion We demonstrated that our Micro-HEP system enables the efficient expression of foreign BGCs, facilitating the discovery of new NPs and increasing yields.

Keywords Heterologous expression, Biosynthetic gene cluster, Transfer, Chassis strain, Integration

*Correspondence:
Gang Li
gang.li@qdu.edu.cn
Jun Fu
fujun@sdu.edu.cn
Ruijuan Li
liruijuan@sdu.edu.cn

Full list of author information is available at the end of the article

Graphical Abstract

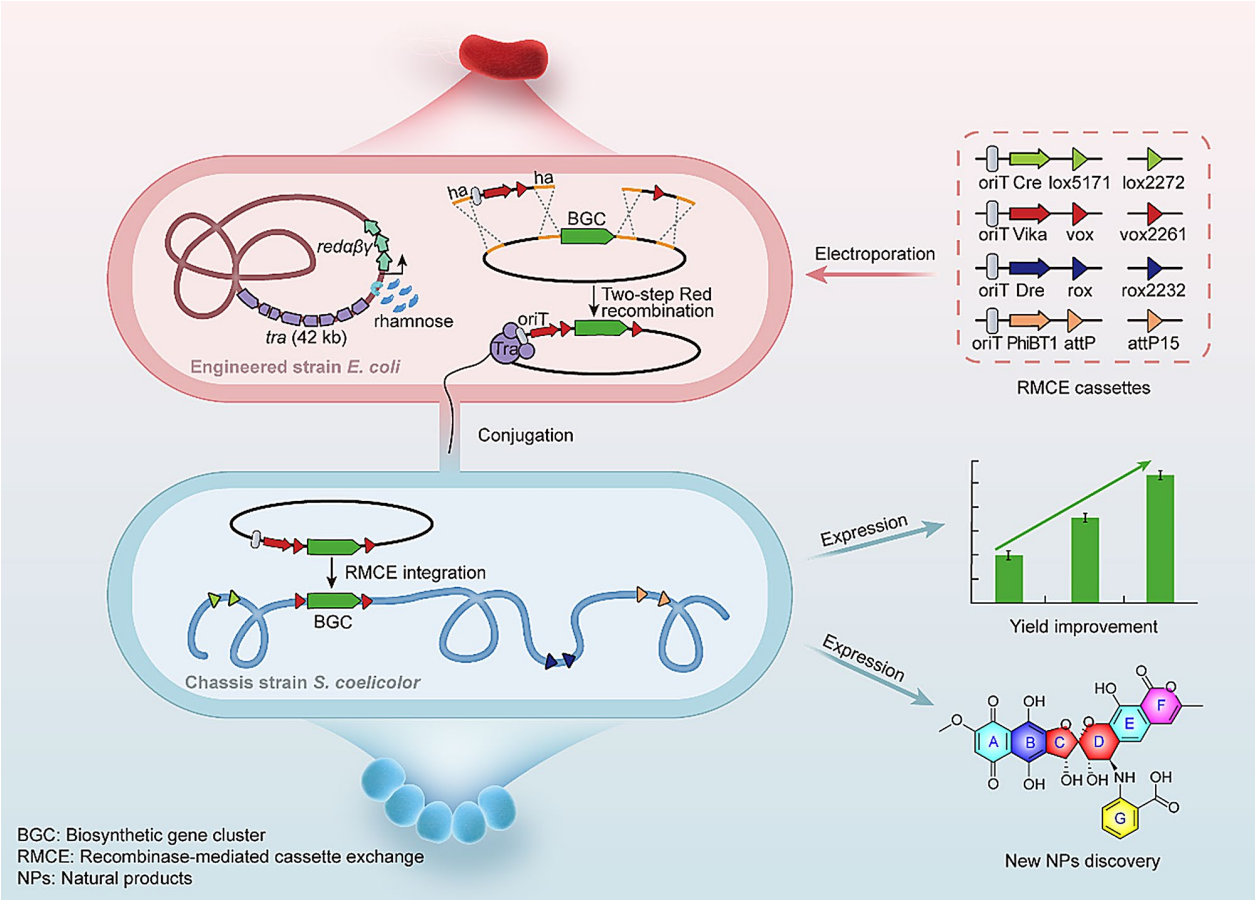

Background

Microbial natural products (NPs) and their derivatives remain indispensable resources in medicine and agriculture, with over 45% of NPs discovered in actinomycetes, predominantly *Streptomyces* [1, 2]. Additionally, with the advancement of high-throughput sequencing and bioinformatics tools, numerous cryptic biosynthetic gene clusters (BGCs) have been found in *Streptomyces*, highlighting the untapped potential of this genus for novel NP discovery [3]. However, a persistent bottleneck in NP application lies in the low production levels of many bioactive NPs in native hosts. Heterologous expression has emerged as a pivotal strategy to circumvent these challenges [4, 5], enabling yield optimization of high-value NPs through pathway engineering, activation of silent BGCs to access chemically diverse metabolites, and mechanistic dissection of biosynthetic pathways [6, 7]. The workflow of heterologous expression generally contains four steps: (1) identifying the BGCs of NPs through bioinformatics analysis of genome sequences, (2) capturing BGCs from genomic DNA by various in vivo or in vitro cloning strategies, (3) modifying BGCs for overexpression by various biotechniques, and (4) transferring and integrating the modified BGCs into the genomes of suitable heterologous hosts for expression [4].

Bioinformatic tools like antiSMASH enable genome mining to predict and analyze BGCs of interest [8]. Transformation-associated recombination (TAR) cloning and exonuclease combined with RecET recombination (ExoCET) can be used to clone BGCs [9, 10], whereas Red recombineering can efficiently modify BGCs. The Red recombination system mediated by λ phage-derived recombinases Redα/Redβ enables precise and efficient DNA editing using short homology arms (50 bp) in *Escherichia coli* [11]. Redα possesses 5'→3' exonuclease activity that generates 3' single-stranded DNA overhangs on double-stranded DNA substrates, and Redβ functions as a single-strand DNA-binding protein that facilitates sequence-specific homologous recombination through annealing of the homology arms. Furthermore, the Redγ protein from λ phage inhibits the ATPase activity of the RecB subunit in the RecBCD nuclease complex, thereby

reducing intracellular degradation of exogenous DNA and enhancing recombination efficiency [11].

Additionally, bacterial conjugation has become a cornerstone strategy for transferring large BGCs from *E. coli* to *Streptomyces*. First described in 1946 as a mechanism of horizontal gene transfer via F plasmid-mediated single-stranded DNA exchange [12], the application of this process was later expanded by the discovery of broad-host-range IncP plasmids, which could mediate DNA transfer not only between Gram-negative bacteria, but also between Gram-negative and Gram-positive bacteria [13]. The *tra* transfer element of IncP plasmids comprises two functional modules: the Tra1 region, encoding the oriT site and DNA processing machinery; and the Tra2 region, mainly responsible for pilus assembly and mating pair formation [14]. *E. coli* ET12567 harboring the IncP plasmid pUZ8002 has been used as a donor for biparental conjugation with *Streptomyces* [15,16]. However, several limitations hinder its broader application, such as low electroporation transformation efficiency, inapplicability of multiplex conjugation due to multiple antibiotic resistance [17] and a lack of correct exconjugants containing large BGCs likely due to instability of repeated sequences [18]. These shortcomings underscore the need for improved conjugation systems for actinomycete genetic manipulation.

Streptomyces species are among the major heterologous hosts, with researchers leveraging the extensive biosynthetic precursor pools and well-established genetic toolkits of these organisms [4, 19]. To minimize native metabolic interference and enhance heterologous pathway flux, a series of *Streptomyces* derivatives with deletions of endogenous BGCs was created by various research groups [20, 21]. Chromosomal amplification of heterologous BGCs represents another key engineering approach for promoting the heterologous expression of BGCs. Many studies have introduced additional $attB_{phiC31}$ sites into *Streptomyces* genomes to enable site-specific integration of multiple-copy BGCs [22–24]. However, recent studies indicate that the introduction of additional $attB_{phiC31}$ sites can reduce the efficiency of DNA transfer and integration [24].

While serine recombinase systems (e.g., PhiC31) dominate *Streptomyces* genome integration, tyrosine recombinases have expanded the genetic toolkit. Established systems, such as Cre/*loxP* (phage P1), Flp/*FRT* (*Saccharomyces* 2μ plasmid), and Dre/*rox* (phage D6), enable marker-free genome editing and large DNA deletions in *Streptomyces* [25, 26]. Notably, the Vika/*vox* system, discovered in 2013 from a *Vibrio coralliilyticus* strain [27], remains unexplored in *Streptomyces*, which represents an untapped opportunity for orthogonal recombination. Tyrosine recombinases exhibit stringent substrate specificity: Cre, Flp, Dre, and Vika exclusively recognize their cognate *loxP*, *FRT*, *rox*, and *vox* sites, respectively, with no cross-reactivity in vivo [27, 28]. Recombination between heterospecific mutant sites (e.g., *lox5171* and *lox2272*) strictly follows the homology-matching principle, with efficient recombination occurring only when the spacer sequences of two sites are identical; for example, *lox5171* and *lox2272* cannot recombine with each other. Leveraging this property, researchers developed recombinase-mediated cassette exchange (RMCE) to enable precise exchange between plasmid-borne target DNA sequences and chromosomal DNA [30]. RMCE offers critical advantages over conventional site-specific recombination; RMCE avoids the integration of plasmid backbones into the genome, thereby minimizing potential disruptions, and RMCE sites stay valid after recombination has taken place, ensuring sustained utility and versatility in genetic engineering applications [31].

Herein, we developed a heterologous expression platform, named Micro-HEP for *micro*bial *h*eterologous *e*xpression *p*latform, which is based on bifunctional engineered strains of *E. coli* and a chassis strain of *S. coelicolor* for the modification, transfer, integration and heterologous expression of BGCs. Central to Micro-HEP is a rhamnose-inducible *redαβγ* recombination system that facilitates precise insertion of RMCE-mediated integration cassettes into BGC-containing plasmids. These cassettes include the transfer origin site oriT, integrase genes, and corresponding recombination target sites (RTSs). The oriT-bearing plasmid is mobilized as single-stranded DNA into the chassis strain *S. coelicolor* A3(2)-2023 via the Tra protein. Finally, the BGCs are integrated into the pre-engineered chromosomal loci by RMCE, bypassing the plasmid backbone. We validated Micro-HEP by expressing two BGCs: the *xim* BGC, responsible for producing the anti-fibrotic xiamenmycin, and the *grh* BGC for producing architecturally complex griseorhodin. Our findings indicate that the Micro-HEP system can facilitate the discovery and production of bioactive NPs with medicinal, agricultural, and industrial applications.

Materials and methods

Strains and plasmids and culture conditions

The strains, plasmids, and antibiotic concentrations used in this study are listed in Table S1, Table S2, and Table S3. *E. coli* strains were cultured in Luria-Bertani (LB) medium (tryptone, 10 g/L; yeast extract, 5 g/L; NaCl, 1 g/L; agar for solid medium, 12 g/L) at 37℃, except for the *E. coli* strains containing the temperature-sensitive plasmid pSC101-P_{Rha}-αβγA-P_{BAD}-ccdA, which were grown at 30 °C. *S. coelicolor* strains were grown in modified soybean-mannitol (MS) medium (defatted soybean meal, 20 g/L; mannitol, 20 g/L; agar, 20 g/L) at 30℃. Glucose yeast-extract maltose (GYM) medium (glucose, 4 g/L; yeast extract, 4 g/L; malt extract 10 g/L) and M1

medium (soluble starch, 10 g/L; yeast extract, 4 g/L; tryptone, 2 g/L) were used for fermentation for the relative quantitative analysis of xiamenmycin and griseorhodin, respectively.

Two-step Red recombination for markerless DNA manipulation in *E. coli*

A counterselectable system and Red recombination were applied to modify genes on *E. coli* chromosomes (Figs. S2A and S2B). The recombinase expression plasmid pSC101-P_{Rha}-αβγA-P_{BAD}-ccdA was electroporated into *E. coli*; in the first round of recombineering, this plasmid was induced dually by 10% L-rhamnose and 10% L-arabinose to express recombinase and CcdA, resulting in replacement of the target gene by an amp-ccdB cassette or kan-rpsL cassette. The kan-rpsL cassette was used to modify the genome of *E. coli* strains GB2005 and GB2006, and the amp-ccdB cassette was used to modify the genome of *E. coli* strains DH5G and S17-1. The correct recombinants were obtained on LB plates containing 10% L-arabinose and antibiotics. In the second round of recombineering, the recombinase expression plasmid was induced to express recombinases by L-rhamnose, and a synthetic oligonucleotide was electroporated into the strain to replace the counterselectable marker cassette. For detailed steps, refer to the section on "Electroporation and recombination in *E. coli*" in the supporting information. All subsequent references to *E. coli* electroporation and recombination in this text follow the methodologies described therein.

Cloning and integration of the conjugative transfer element and recombinase genes (tra-P_{Rha}-redαβγ) in *E. coli*

The element tra-P_{Rha}-redαβγ was integrated into the genome of *E. coli* using the Gateway system. Firstly, the DNA fragment attB1-cm-attB2, which contained attB sites (recognized by the Int_{λ} integrase) and 50-bp homology arms, was inserted into the target region of the *E. coli* chromosome by Red recombination. The correct recombinants were selected on LB plates containing 15 mg/mL chloramphenicol. Next, the plasmid p15A-amp-ccdB-int_{λ}-attP1-zeo-tra-P_{Rha}-αβγ-attP2, assembled by ExoCET [9], was transferred to the above correct recombinants, and the strains were allowed to recover at 30℃ for 2.5 h and then spread on LB plates containing 15 mg/mL zeocin. Single colonies were replica-patched onto LB plates with 15 mg/mL zeocin and LB plates with 15 mg/mL chloramphenicol. The colonies that grew only on the plates with zeocin were further verified by colony PCR using the indicated primers to check for tra-P_{Rha}-redαβγ integration into the following sites of the recombinants: *ybcW* position, primers ybcW-F-1/F-2 and R-1/ybcW-R-2; *pspG* position, primers pspG-F-1/F-2 and R-1/pspG-R-2; *recET* position, primers recET-F-1/F-2 and R-1/recET-R-2; and *yfiM* position, primers yfiM-F-1/F-2 and R-1/yfiM-R-2. Primers are shown in the Table S4.

Intergeneric conjugation

Intergeneric conjugation between *E. coli* and *S. coelicolor* was performed as described previously [16, 32] with minor modifications. An overnight culture of the donor *E. coli* with the plasmid containing the BGC was diluted 10-fold in 10 mL fresh LB plus 10 mg/mL apramycin and grown at 37℃ until the OD_{600} reached 0.6. The donor cells were washed twice and resuspended in 10 mL ddH_2O. Spores of the *S. coelicolor* strain to be used as the recipient were harvested in 8 mL of 2× yeast extract-tryptone (2×YT) medium (tryptone, 16 g/L; yeast extract, 10 g/L; NaCl, 5 g/L) from an SM plate and were induced to germinate by heat shock (50℃, 10 min) and ice bath (4℃, 5 min). Donors (3 mL) and recipients (1 mL) were mixed, and then, the mixture was spread on MS plates containing 10 mM $MgCl_2$ and cultivated at 30℃. After 17 h, the plates were overlaid with 1 mL of sterile water containing 20 mg/mL apramycin and 50 mg/mL nalidixic acid and further cultivated at 30℃ until exconjugant colonies appeared.

Construction of the chassis strain *S. coelicolor* A3(2)-2023

The plasmid pKC1139-red-vox-apra-vox2261 was introduced into the strain *S. coelicolor* A3(2) by conjugation, and successful exconjugants were obtained based on their ability to grow on MS agar plates supplemented with 20 mg/mL apramycin. Exconjugants were cultivated at 39℃ to promote recombination. Single colonies were obtained and replica-patched onto MS plates with 20 mg/mL apramycin and MS plates with 25 mg/mL thiostrepton. The growth of colonies only in MS plates with apramycin indicated that the *red* BGC in the chromosome of *S. coelicolor* was replaced with vox-lox71-apra-lox66-vox2261 using a double-crossover approach, resulting in strain *S. coelicolor* A3(2)-red-apra. Then, pUWLCRE [24], which can express the recombinase gene *cre*, was introduced into *S. coelicolor*-red-apra by conjugation, and exconjugants were selected using 25 mg/mL thiostrepton-supplemented MS agar plates. Exconjugants were cultivated at 30℃ in liquid TSB medium with 25 mg/mL thiostrepton, and the cultures were spread onto MS plates with no antibiotics to obtain single colonies, which were then replica-patched onto MS plates without antibiotics and with 20 mg/mL apramycin. Colonies that grew only on MS plates without antibiotics were verified by colony PCR using primers red-vox-1/red-vox2261-2 and sequence analysis, with the resulting strain named *S. coelicolor* A3(2)-1.

S. coelicolor A3(2)-2, *S. coelicolor* A3(2)-3, *S. coelicolor* A3(2)-4, and *S. coelicolor* A3(2)-2023 were constructed using plasmids pKC1139-act-rox-apra-rox2232,

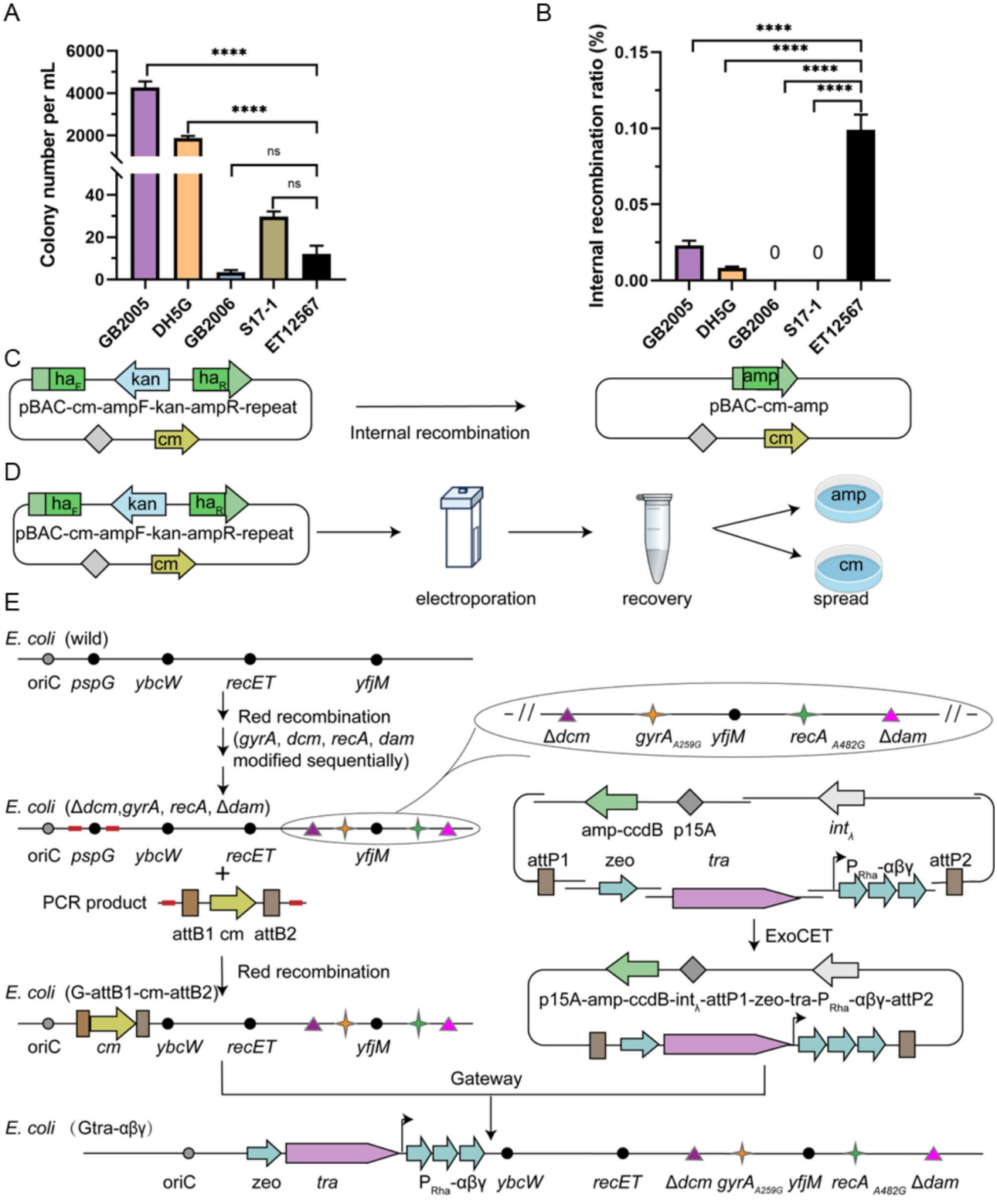

Fig. 1 (See legend on next page.)

(See figure on previous page.)

Fig. 1 Construction of the DNA modification and conjugation transfer system tra-P_{Rha}-redαβγ in *E. coli* strains. (**A**) Electroporation transformation efficiency of four parental *E. coli* strains (GB2005, DH5G, GB2006 and S17-1) and the control strain ET12567 were as determined by the number of colonies grown after transfer of the plasmid pBAC-sal-phiC31-apra-oriT (116 kb). (**B**) Internal recombination ratio of plasmid pBAC-cm-ampF-kan-ampR-repeat in five *E. coli* strains. The internal recombination ratio was defined as the colony number on LB plates containing ampicillin divided by the number on LB plates containing chloramphenicol. In *E. coli* GB2006 and S17-1, the internal recombination ratio of the plasmid was determined to be zero. For (A, B) error bars indicate SD; $n = 3$; ns, $p > 0.05$; ****$p < 0.0001$. (**C**) Diagrams of plasmids pBAC-cm-ampF-kan-ampR-repeat and pBAC-cm-amp. Plasmid pBAC-cm-ampF-kan-ampR-repeat contains two 500-bp homologous arms (haF and haR) flanking the *kan* cassette. Critically, haF and haR (dark green) are truncated, non-functional fragments of the ampicillin resistance gene (*amp*). Homologous recombination between these arms excises the intervening *kan* cassette while reconstituting a functional *amp* through precise end-joining (pBAC-cm-amp). (**D**) Schematic diagram of workflow for comparing internal recombination ratios. (**E**) Construction strategy for engineering the *E. coli* strains. Firstly, the *gyrA*, *dcm*, *recA*, and *dam* genes were modified sequentially, and then, the attB1-cm-attB2 cassette was inserted into a target location (e.g., *pspG*) on the *E. coli* chromosome by Red recombination. Finally, the attB1-cm-attB2 cassette was replaced by the element tra-P_{Rha}-redαβγ.

pYH7-cda-lox5171-apra-lox2272, pYH7-attB$_{phiBT1}$-FRT-apra-F3, and pYH7-clb-attB-apra-attB15, respectively, and were verified by colony PCR using primers act-rox-1/act-rox2232-2, cda-lox5171-1/cda-lox2272-2, attB-FRT-1/attB-F3-2, and clb-attB-1/clb-attB-2, respectively. The construction procedure was similar to that used for *S. coelicolor* A3(2)-1. All mutant strains were purified through three rounds of single-spore isolation on SM agar prior to phenotypic characterization, as described [33].

Relative quantitative analysis of the production of xiamenmycin and KS-619-1

S. coelicolor strains containing one or multiple copies of the *xim* BGC were grown in 30 mL of tryptic soy broth (TSB) medium (Hopebio, Qingdao, China) for 2 days. Then, 1 mL of seed culture was inoculated into 50 mL GYM medium in a 250 mL shake flask and cultivated at 30℃, 200 rpm. On the seventh day, absorber resin Amberlite XAD-16 was added followed by incubation for 18 h. The crude extracts (the biomass and XAD-16) were extracted with 30 mL methanol. Finally, extracts were subjected to evaporation and dissolved in 1 mL methanol.

The fermentation procedure used for *S. coelicolor* strains containing the *grh* BGC was similar to that used for the strain containing *xim* BGC. The fermentation medium was M1 medium, and 1 mL fermentation samples were harvested at 2, 3, 4, and 5 days and dissolved in 1 mL methanol after freeze-drying.

For HPLC, 5 μL crude extracts were analyzed: water with 0.1% (v/v) TFA: acetonitrile (ACN) gradient was used as the mobile phase for 0–3 min, 5% ACN; 3–18 min, 5–95% ACN; 18–22 min, 100% ACN; and 22–25 min, 5% ACN by UV spectroscopy at 190–400 nm. The peak area was used to compare product yields by UV spectroscopy at 254 nm.

Results

Construction of the engineered *E. coli* strains with DNA modification and conjugative transfer system (tra-P_{Rha}-redαβγ)

E. coli GB05-red is commonly used for the modification of BGCs by the recombination system Redαβγ, whereas *E. coli* ET12567 (pUZ8002) [16] and *E. coli* S17-1 [34] are used in conjugative transfer systems for transferring plasmids containing oriT and BGCs to *Streptomyces*. At present, there is no engineered *E. coli* strain that can be used to both modify DNA and then transfer that DNA to *Streptomyces.* Therefore, we looked for *E. coli* strains that had both capacities as well as other key features.

Since electroporation transformation efficiency is critical for efficient recombineering in *E. coli* [35], we evaluated the efficiency of several laboratory strains of *E. coli* and found that strains DH5G and GB2005 exhibited the highest electroporation transformation efficiency among these strains (Fig. 1A).

Sequence stability was also an important consideration in our choice of *E. coli* strains due to the inherent instability of repetitive sequences within NP BGCs, particularly in BGCs for polyketide synthases (PKSs) [36]. We established a plasmid-based recombination reporter system (pBAC-cm-ampF-kan-ampR-repeat) to systematically evaluate repetitive sequence stability through quantification of intramolecular recombination efficiency of the plasmid (Fig. 1B, C and D). The plasmid contains 500 bp-long homologous repeat units (non-functional fragments: haF and haR) of the ampicillinresistance gene (*AmpR*) flanking the kanamycin resistance gene (*KanR*) to form recombination-sensitive cassettes. Plasmid stability was assessed through a dual-resistance phenotypic assay: intact plasmids conferred chloramphenicol (*CmR*) and *KanR* resistance, whereas homologous recombination between repeats excised *kanR*, resulting in *CmR* and *AmpR*. Quantified as the internal recombination ratio (AmpR/CmR), higher values indicated greater sequence instability. Strikingly, GB2006 and S17-1 exhibited undetectable recombination (ratio = 0), while GB2005 and DH5G demonstrated significantly lower ratios when compared to ET12567 (Fig. 1B). The TFIIA cosmid,

which harbored 17 pairs of repetitive sequences (each pair length > 30 bp), could also replicate stably in GB2006, S17-1, and DH5G (Fig. S1A). The stable existence of repetitive sequences in *E. coli* is conducive to the cloning and modification of large BGCs. The above results indicated that the four *E. coli* strains GB2005, DH5G, GB2006, and S17-1 were promising candidates for the development of efficient systems for DNA modification and conjugative transfer.

To engineer an optimal donor strain of *E. coli*, we modified the *gyrA*, *recA*, *dcm*, and *dam* genes by Red recombination combined with counterselection, eliminating intrinsic antibiotic resistance and methylation-based restriction barriers (*SI Appendix*, Results, Fig. 1E and Fig. S2). *E. coli* S17-1 contains an active bacteriophage Mu genome, which can mobilize itself into recipient strains at a certain frequency [38]. For efficient transfer of mobilizable plasmids without the transfer of chromosomal genes, the Mu genome was deleted, constructing the Mu-free donor strain S17-1ΔMu (Table 1).

Additionally, the dual-function element tra-P_{Rha}-redαβγ, comprising the Red recombination system and Tra conjugative transfer system, was assembled onto plasmid p15A-amp-ccdB-int_{λ}-attP1-zeo-tra-P_{Rha}-αβγ-attP2 by ExoCET (Fig. S3A) for subsequent chromosomal integration into *E. coli* strains. This p15A-based plasmid contains the *ccdB* gene, which encodes a toxic protein that is used for counterselection against maintenance of the whole plasmid. The attP sites on the plasmid are recombined with the attB sites on chromosome of *E. coli* by integrase Int_{λ}, that is used for chromosomal integration of element tra-P_{Rha}-redαβγ.

The position of genes on the chromosome critically affects their expression level in *E. coli* [37]. To investigate whether chromosomal position influences conjugation frequency, we selected four chromosomal conserved sites for insertion of the dual-function element in *E. coli* strains GB2005, GB2006, and DH5G. The following positions were selected based on their distance to chromosomal oriC: the *yfjM* gene of prophage CP4-57, the *ybcW* gene of prophage DLP12, and genes *pspG* and *recET*. Using the Gateway system, tra-P_{Rha}-redαβγ (45 kb) was inserted into the chosen locations on the chromosomes (Fig. 1E) with verification by PCR (Fig. S3B). No correct clone was obtained at the *ybcW* site in GB2005, and so, eleven engineered strains were obtained based on the three *E. coli* strains and four different positions: four derivatives of DH5G (DH5G-CP4-57tra-αβγ, DH5G-DLP12tra-αβγ, DH5G-Gtra-αβγ, and DH5G-recETtra-αβγ); four derivatives of GB2006 (GB06-CP4-57tra-αβγ, GB06-DLP12tra-αβγ, GB06-Gtra-αβγ, and GB06-recETtra-αβγ); and three derivatives of GB2005 (GB05-CP4-57tra-αβγ, GB05-Gtra-αβγ, and GB05-recETtra-αβγ) (Table 1).

Table 1 Genotype of engineered strains

Strains	Genotype
GB05-Gtra-αβγ	GB2005, Δ*dcm*(G135A), *recA*(A482G), Δ*dam*, *pspG*::(tra-P_{Rha}-redαβγ)
GB05-CP4-57tra-αβγ	GB2005, Δ*dcm*(G135A), *recA*(A482G), Δ*dam*, *yfjM*::(tra-P_{Rha}-redαβγ)
GB05-recETtra-αβγ	GB2005, Δ*dcm*(G135A), *recA*(A482G), Δ*dam*, *recET*::(tra-P_{Rha}-redαβγ)
GB06-Gtra-αβγ	GB2006, *gyrA*(A259G), Δ*dcm*(G135A), *recA*(A482G), Δ*dam*, *pspG*::(tra-P_{Rha}-redαβγ)
GB06-CP4-57tra-αβγ	GB2006, *gyrA*(A259G), Δ*dcm*(G135A), *recA*(A482G), Δ*dam*, *yfjM*::(tra-P_{Rha}-redαβγ)
GB06-DLP12tra-αβγ	GB2006, *gyrA*(A259G), Δ*dcm*(G135A), *recA*(A482G), Δ*dam*, *ybcW*::(tra-P_{Rha}-redαβγ)
GB06-recETtra-αβγ	GB2006, *gyrA*(A259G), Δ*dcm*(G135A), *recA*(A482G), Δ*dam*, *recET*::(tra-P_{Rha}-redαβγ)
DH5G-Gtra-αβγ	DH5G, *gyrA*(A259G), Δ*dcm*(G135A), *recA*(A482G), Δ*dam*, *pspG*::(tra-P_{Rha}-redαβγ)
DH5G-CP4-57tra-αβγ	DH5G, *gyrA*(A259G), Δ*dcm*(G135A), *recA*(A482G), Δ*dam*, *yfjM*::(tra-P_{Rha}-redαβγ)
DH5G-DLP12tra-αβγ	DH5G, *gyrA*(A259G), Δ*dcm*(G135A), *recA*(A482G), Δ*dam*, *ybcW*::(tra-P_{Rha}-redαβγ)
DH5G-recETtra-αβγ	DH5G, *gyrA*(A259G), Δ*dcm*(G135A), *recA*(A482G), Δ*dam*, *recET*::(tra-P_{Rha}-redαβγ)
S17-1Δmu	S17-1, Δ*dcm*(G135A), *recA*(C233T), Δ*dam*, ΔMu

Characterization of the engineered *E. coli* strains with DNA modification and conjugative transfer system (tra-P_{Rha}-redαβγ)

The versatility of the tra-P_{Rha}-redαβγ modification and conjugative transfer system in *E. coli* was assessed by conjugation frequency, electroporation efficiency, recombination efficiency, and stability of repetitive sequences (Fig. 2).

The conjugation frequency of plasmid pBAC-sal-phiC31-apra-oriT, which contains a 106 kb salinomycin BGC, PhiC31 integrase gene, and *attP* site, was tested between the donor *E. coli* and recipient *S. coelicolor* A3(2). Exconjugants of *S. coelicolor* were obtained by intrageneric conjugation from the twelve engineered *E. coli* strains (Table 1) and the control strain *E. coli* ET12567 (pUZ8002). Conjugation frequency was calculated as the number of exconjugants divided by the number of *S. coelicolor* spores. The *E. coli* GB2005-derived strains containing the *tra* system were the most efficient at transferring the plasmid to the recipient *S. coelicolor* A3(2), with transfer frequencies between approximately 9.2×10^{-5} and 1.8×10^{-4} (Fig. 2A). The highest transfer frequency was obtained with *tra* inserted into the *recET* site of GB2005 (*E. coli* GB05-recETtra-αβγ), which yielded a 2-fold higher frequency compared with that of *E. coli* ET12567 (pUZ8002) system, which had a transfer frequency of 9.0×10^{-5}. With the DH5G-derived strains as the donor strains, the frequency of conjugation transfer was between 1.7×10^{-6} and 6.0×10^{-6}, which is 15–53

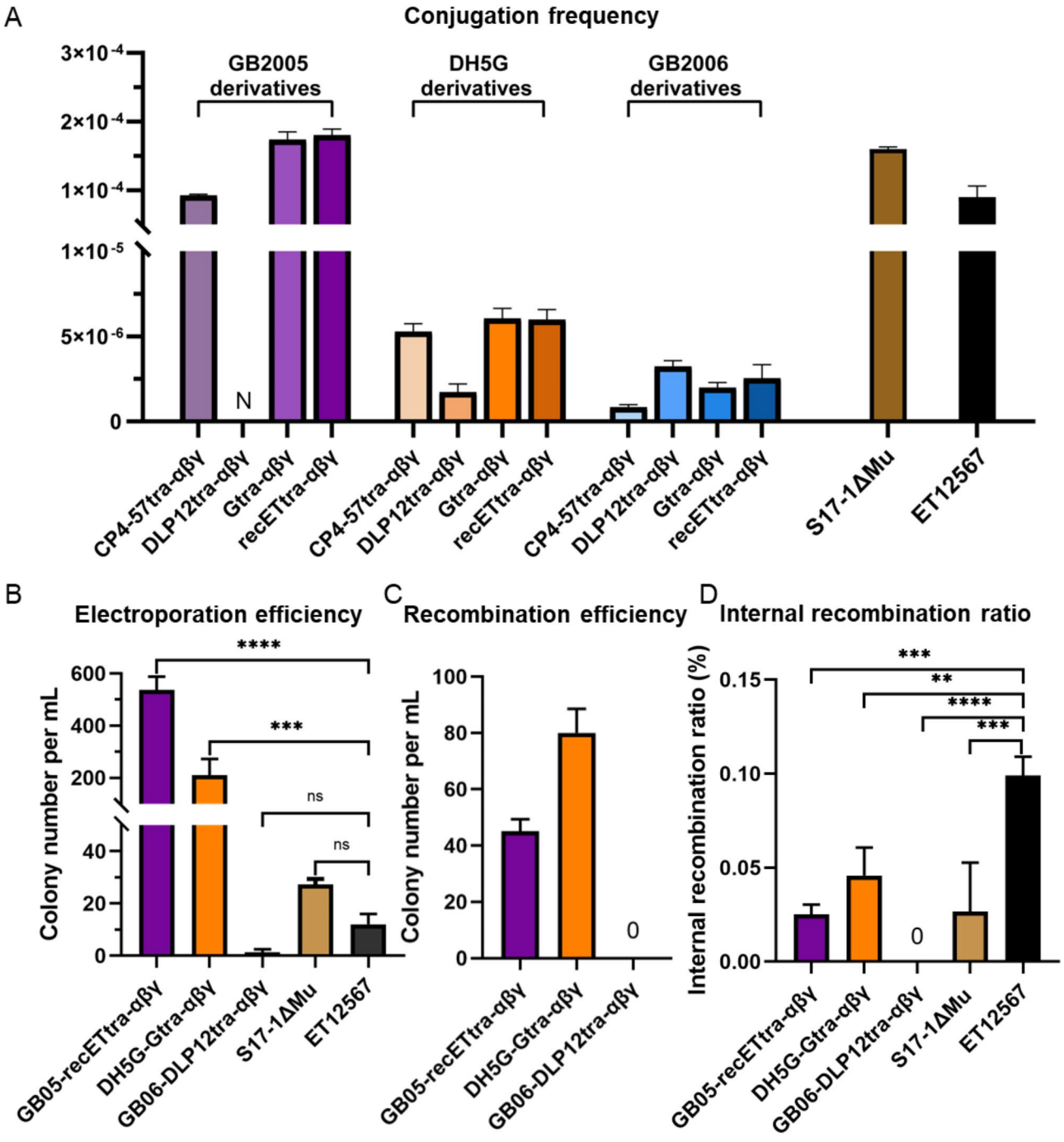

Fig. 2 Characterization of the engineered *E. coli* strains. (**A**) Conjugation frequency of plasmid pBAC-sal-phiC31-apra-oriT in transfer from eleven engineered *E. coli* strains to *S. coelicolor* A3(2). Three of the engineered strains were derivatives of *E. coli* GB2005 (purple), with four engineered strains derived each from *E. coli* DH5G (orange) and *E. coli* GB2006 (blue). N represents no data. (**B**) Electroporation efficiency of four engineered strains and *E. coli* ET12567 as determined by the number of colonies grown after transfer of plasmid pBAC-sal-phiC31-apra-oriT (116 kb). (**C**) Recombination efficiency of *E. coli* GB05-recETtra-αβγ, DH5G-Gtra-αβγ, and GB06-DLP12tra-αβγ. The correct recombinant was not obtained in GB06-DLP12tra-αβγ. (**D**) Internal recombination ratio of pBAC-cm-ampF-kan-ampR-repeat in four engineered *E. coli* strains and ET12567. Error bars, SD; $n = 3$; ns, $p > 0.05$; ** $p < 0.01$; *** $p < 0.001$; **** $p < 0.0001$

times lower than the level for ET12567 (pUZ8002); the highest transfer frequency among the DH5G-derived strains was obtained with DH5G-Gtra-αβγ, which has *tra* inserted into the *pspG* site (Fig. 2A). The transfer frequency with GB2006-derived strains was similar to that of the DH5G derivates (0.8×10^{-6} and 3.2×10^{-6}), and the DLP12 prophage *ybcW* gene was the optimal site for *tra* insertion with this set (Fig. 2A). With *E. coli*

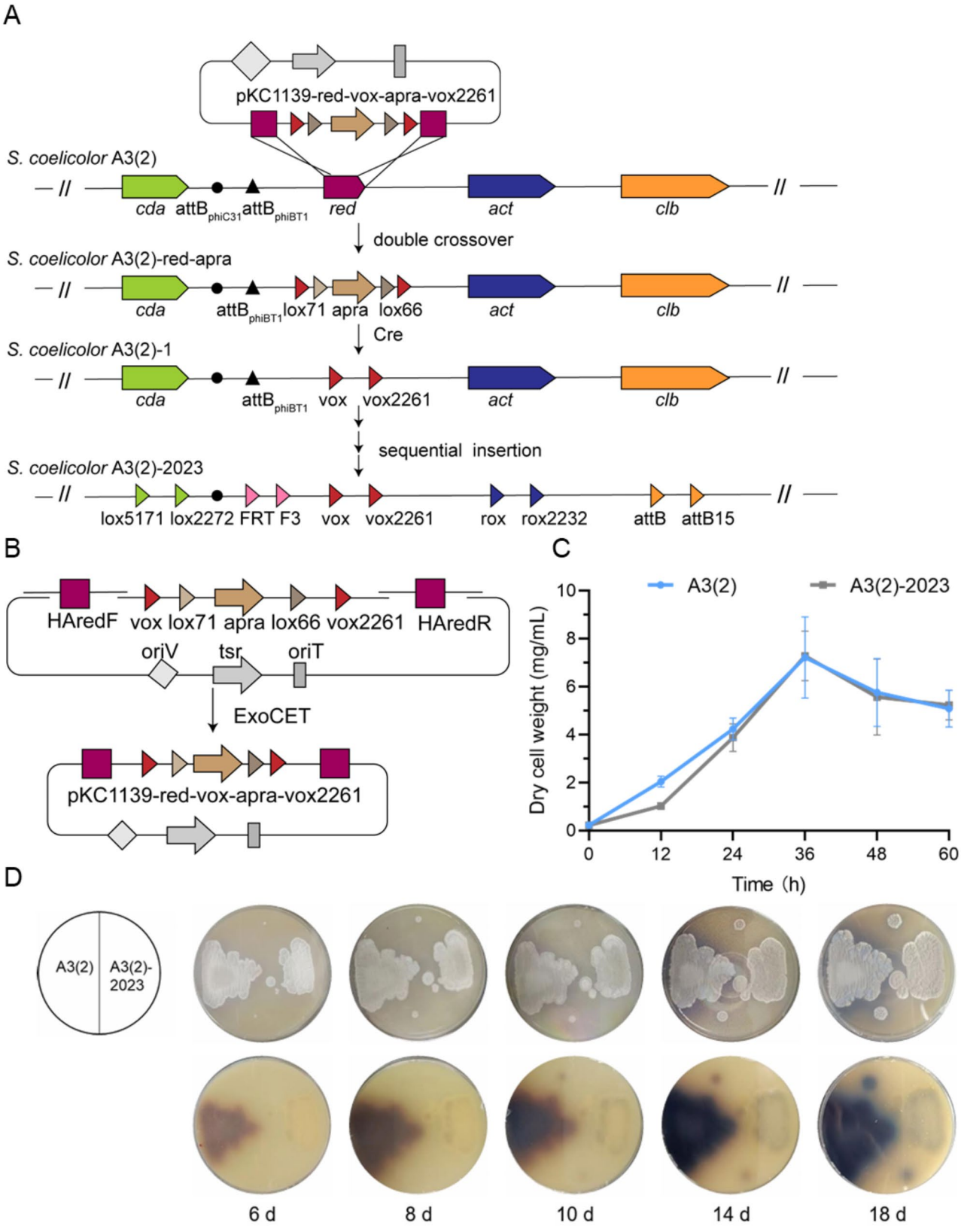

Fig. 3 (See legend on next page.)

(See figure on previous page.)

Fig. 3 Construction and growth studies of the chassis strain *S. coelicolor* A3(2)-2023. (**A**) The overall strategy for the construction of the chassis strain *S. coelicolor* A3(2)-2023 using a double-crossover approach and Cre-mediated site-specific recombination. The targeted endogenous *red* BGC was replaced with vox-lox71-apra-lox66-vox2261 by a double crossover. Sites *lox71* and *lox66* were recombined by Cre to eliminate the apramycin resistance gene. *S. coelicolor* A3(2)-2023 was constructed with five RMCE sites (vox-vox2261, rox-rox2232, lox5171-lox2272, FRT-F3, and attB-attB15) sequentially inserted into the chromosome of *S. coelicolor* A3(2). (**B**) Construction of the knockout plasmid pKC1139-red-vox-apra-vox2261. The resulting plasmid was used for *red* BGC knockout and vox-vox2261 site insertion on the *S. coelicolor* A3(2) chromosome. (**C**) Growth curves of *S. coelicolor* A3(2) and *S. coelicolor* A3(2)-2023 in TSB liquid medium. (**D**) Growth and sporulation of *S. coelicolor* A3(2) and *S. coelicolor* A3(2)-2023 on MS agar medium. The color of the MS agar medium with *S. coelicolor* A3(2) was initially red due to the production of prodiginines (red complex) and then turned to blue upon the production of actinorhodin (blue product)

S17-1ΔMu as the donor strain, the frequency of exconjugant formation was 1.6×10^{-4}, which is also higher than the frequency with ET12567 (pUZ8002).

Our results demonstrated that the parental strain and the insertion location of *tra* affected the conjugative transfer frequency and that the parental source of the derived strain may be the main factor. Although the optimal sites of *tra* insertion in three *E. coli* were different, strains with *tra* insertion in the *recET* site all obtained a high conjugation transfer frequency. Thus, the *recET* site is a potential site for inserting large DNA fragments. The four *E. coli* engineered strains GB05-recETtra-αβγ, DH5G-Gtra-αβγ, GB06-DLP12tra-αβγ and S17-1ΔMu, which had the highest conjugation transfer frequency among each set of strains, were selected for further study. The growth curves of these four engineered *E. coli* strains and ET12567 are shown in Fig. S4. Except for GB05-recETtra-αβγ, the biomass of our engineered strains was similar to or higher than that of ET12567.

The variation in electroporation efficiency is solely attributable to the genetic background of the *E. coli* strains, not the chromosomal integration site of the tra-P_{Rha}-redαβγ. Based on their high conjugation efficiency within their respective parental strain lineages, the four engineered strains (GB05-recETtra-αβγ, DH5G-Gtra-αβγ, GB06-DLP12tra-αβγ, and S17-1ΔMu) were selected for comparison of electroporation efficiency. The electroporation efficiency of GB05-recETtra-αβγ, DH5G-Gtra-αβγ, and S17-1ΔMu was 42-fold, 18-fold, and 2-fold higher than that of the control strain ET12567 using plasmid pBAC-sal-phiC31-apra-oriT, respectively (Fig. 2B). In contrast, the electroporation efficiency of GB06-DLP12tra-αβγ was 9-fold lower than that of ET12567.

The rhamnose-inducible promoter P_{Rha} stringently and efficiently induces expression of the recombination system Redαβγ in *E. coli* [39]. The recombination efficiency between linear and circular DNA in GB05-recETtra-αβγ, DH5G-Gtra-αβγ, and GB06-DLP12tra-αβγ was tested using the plasmid modification assay, which uses a PCR product containing the ampicillin resistance gene and the PhiBT1 integrase gene flanked by 80-bp homology arms to replace the PhiC31 integrase gene on plasmid pBAC-sal-phiC31-apra-oriT (Fig. S5). The correct recombinants were obtained in both DH5G-Gtra-αβγ and GB05-recETtra-αβγ, with 80 and 45 recombinant colonies per milliliter, respectively; however, recombinants were not obtained with GB06-DLP12tra-αβγ (Fig. 2C). Based on the above findings, strains GB05-recETtra-αβγ and DH5G-Gtra-αβγ appeared optimal for further modification of large BGCs and mobilization of BGCs for transfer to *Streptomyces*.

Finally, the internal recombination ratio for plasmid pBAC-cm-ampF-kan-ampR-repeat (Fig. 1C and D) was used to assess the stability of repetitive sequences in the engineered *E. coli* strains, with remarkable stability displayed in GB06-DLP12tra-αβγ (Fig. 2D). The stability of the repetitive sequences in GB05-recETtra-αβγ, S17-1ΔMu, and DH5G-Gtra-αβγ was also better than in ET12567 (Fig. 2D).

After comprehensive consideration of the conjugation transfer frequency, electroporation efficiency, and recombination efficiency, we selected the engineered strain *E. coli* GB05-recETtra-αβγ for modification and transfer of BGCs. However, for BGCs containing multiple repetitive sequences, strain GB06-DLP12tra-αβγ would be an alternative.

Construction of the chassis strain *S. coelicolor* A3(2)-2023 with multiple RMCE sites

Based on the hypothesis that "chromosome natural secondary metabolic BGC sites are more conducive to foreign BGC expression", four endogenous BGCs were chosen to be replaced by RMCE sites within the chromosome of *S. coelicolor* A3(2), including the prodiginine (*red*), actinorhodin (*act*), calcium-dependent antibiotic (*cda*), and coelibactin (*clb*) BGCs. The overall strategy for the construction of the marker-free chassis strain *S. coelicolor* A3(2)-2023 involved a combination of homologous recombination and site-specific recombination, with the latter mediated by the Cre/*lox* system (*SI Appendix*, Results, Fig. 3A and B and S6). The introduced RMCE sites were verified by PCR and sequence analysis (Fig. S7). In this manner, the five RMCE sites vox-vox2261, rox-rox2232, lox5171-lox2272, FRT-F3, and attB-attB15 were sequentially inserted into the BGCs for *red*, *act*, and *cda*, the natural $attB_{phiBT1}$ site, and BGC *clb* in the *S. coelicolor* A3(2) chromosome (Fig. 3A and Fig. S6). The final chassis strain was designated *S. coelicolor* A3(2)-2023, which lacked the four BGCs through deletion of 159 kb

of the chromosome and had five introduced RMCE sites (Table S5).

In TSB liquid medium, the chassis strain *S. coelicolor* A3(2)-2023 exhibited no significant differences in growth when compared with the wild-type strain *S. coelicolor* A3(2) (Fig. 3C). However, the major secondary metabolites of *S. coelicolor* A3(2), the prodiginines (red complex) and actinorhodin (blue product), were not produced due to deletion of the *red* and *act* BGCs (Fig. 3D). These deletions resulted in a cleaner metabolic background for *S. coelicolor* A3(2)-2023 compared with that of the wild-type strain.

Establishment of a RMCE system to mediate integration of the BGC into*S. coelicolor* A3(2)-2023

To determine whether the five introduced RMCE sites and corresponding integrases have the capability to mediate integration of foreign BGCs into the *S. coelicolor* A3(2)-2023 chromosome, the xiamenmycin (*xim*) BGC from *S. xiamenensis* 318 [40] was selected as a foreign BGC for integration into the each of the five RMCE sites on the chromosome (Fig. 4A and Table S6). Five integrative vectors with *xim* BGC were constructed and verified by restriction endonucleases analysis (Fig. 4B and Fig. S8A). Four correct exconjugants containing one copy of the *xim* BGC (*S. coelicolor* vox-xim-vox2261, rox-xim-rox2232, lox5171-xim-lox2272, and attB-xim-attB15) were obtained by Vika-, Dre-, Cre- and PhiBT1-mediated RMCE integration, respectively. Then, three exconjugants containing multiple copies of the *xim* BGC (*S. coelicolor* xim-2copies, xim-3copies, xim-4copies-apra) were also obtained (Fig. 4A). All of the strains were verified by colony PCR (Fig. S8B). However, no correct exconjugant was obtained by Flp-mediated RMCE recombination, possibly due to its low integrase activity.

Analysis by high-performance liquid chromatography–mass spectrometry (HPLC-MS) demonstrated that all four exconjugants containing one copy of the *xim* BGC could produce xiamenmycin in GYM medium (Figs. S8C, S8D, and S8E). The expression levels of the above four exconjugants were tested through relative quantitative analysis by HPLC. In comparison to strain *S. coelicolor* xim-attB$_{phiC31}$, which has *xim* BGC integrated into the attB$_{phiC31}$ site of *S. coelicolor* A3(2)-2023 and which was used as a control, production of xiamenmycin by the exconjugant *S. coelicolor* lox5171-xim-lox2272 was 1.57-fold higher (Fig. 4C). These results demonstrated that the location of the *xim* BGC within the *S. coelicolor* A3(2)-2023 chromosome could affect the expression level. HPLC results showed that the production of xiamenmycin was also enhanced by increasing the copy numbers of the *xim* BGC (Fig. 4C). As the number of copies of the BGC increased from 2 to 4, the yield of xiamenmycin increased from 1.92 to 5.52-fold compared with the control level (Fig. 4C). Using our RMCE system, we successfully integrated four copies of the *xim* BGC into the *S. coelicolor* A3(2)-2023 chromosome and achieved highly efficient expression of xiamenmycin. The above results indicated that RMCE systems can mediate the multicopy chromosomal integration of natural product BGCs into *S. coelicolor* A3(2)-2023 and facilitate the production of NPs.

Heterologous expression of the type II polyketide BGC *grh* using Micro-HEP based on *E. coli* GB05-recETtra-αβγ and*S. coelicolor* A3(2)-2023

antiSMASH analysis indicated that the type II polyketide BGC *grh* from *Streptomyces* sp. LS-1 (GenBank accession no. CP141946) was highly similar to the BGC for griseorhodins, which belong to a growing family of rubromycins [41]. The naturally occurring rubromycins have gathered considerable attention due to their notable biological functions, including antimicrobial, anticancer, and enzyme inhibitory activities. However, isolation and structural elucidation of these compounds have been challenging due to their complex structures and low yields [42]. Therefore, we expressed *grh* BGC using Micro-HEP (Fig. 5A). The BGC *grh* was integrated separately into the attB$_{phiC31}$ site and vox-vox2261 site of the chassis strain *S. coelicolor* A3(2)-2023 as well as into the attB$_{phiC31}$ site of wild-type *S. coelicolor* A3(2). Moreover, the BGC integration efficiency remains 100% regardless of BGC size—both the 7.5 kb *xim* and 90 kb *grh* BGCs showed precise RMCE integration in all exconjugants analyzed ($n = 12$ per BGC). The exconjugants *S. coelicolor* A3(2)-2023-grh-attB$_{phiC31}$, A3(2)-2023-vox-grh-vox2261, and A3(2)-grh-attB$_{phiC31}$ were obtained and fermented in M1 media.

LC-MS analysis results showed that there were several new peaks in *S. coelicolor* A3(2)-2023-grh-attB$_{phiC31}$ compared with the control strain *S. coelicolor* A3(2)-grh-attB$_{phiC31}$, such as compound **3** (Fig. 5B). The area of the most abundant peak (compound **2**) at 16 min was used to compare the expression level of the *grh* BGC in different strains. The results showed that *S. coelicolor* A3(2)-2023-grh-attB$_{phiC31}$ and *S. coelicolor* A3(2)-2023-vox-grh-vox2261 produced, respectively, 3.4- and 2.9-fold higher quantities of compound **2** compared with levels in *S. coelicolor* A3(2)-grh-attB$_{phiC31}$ by the fourth day (Fig. 5C). The expression level of the *grh* BGC in the chassis strain *S. coelicolor* A3(2)-2023 was higher than in the *S. coelicolor* A3(2) strain, suggesting that deletion of the *act* BGC (type II PKS product) in the chassis strain reduced competition for precursors. Increasing the copy number of BGC had limited effect on the production of compound **2** (Fig. S9). However, other metabolic engineering strategies could be considered to further improve

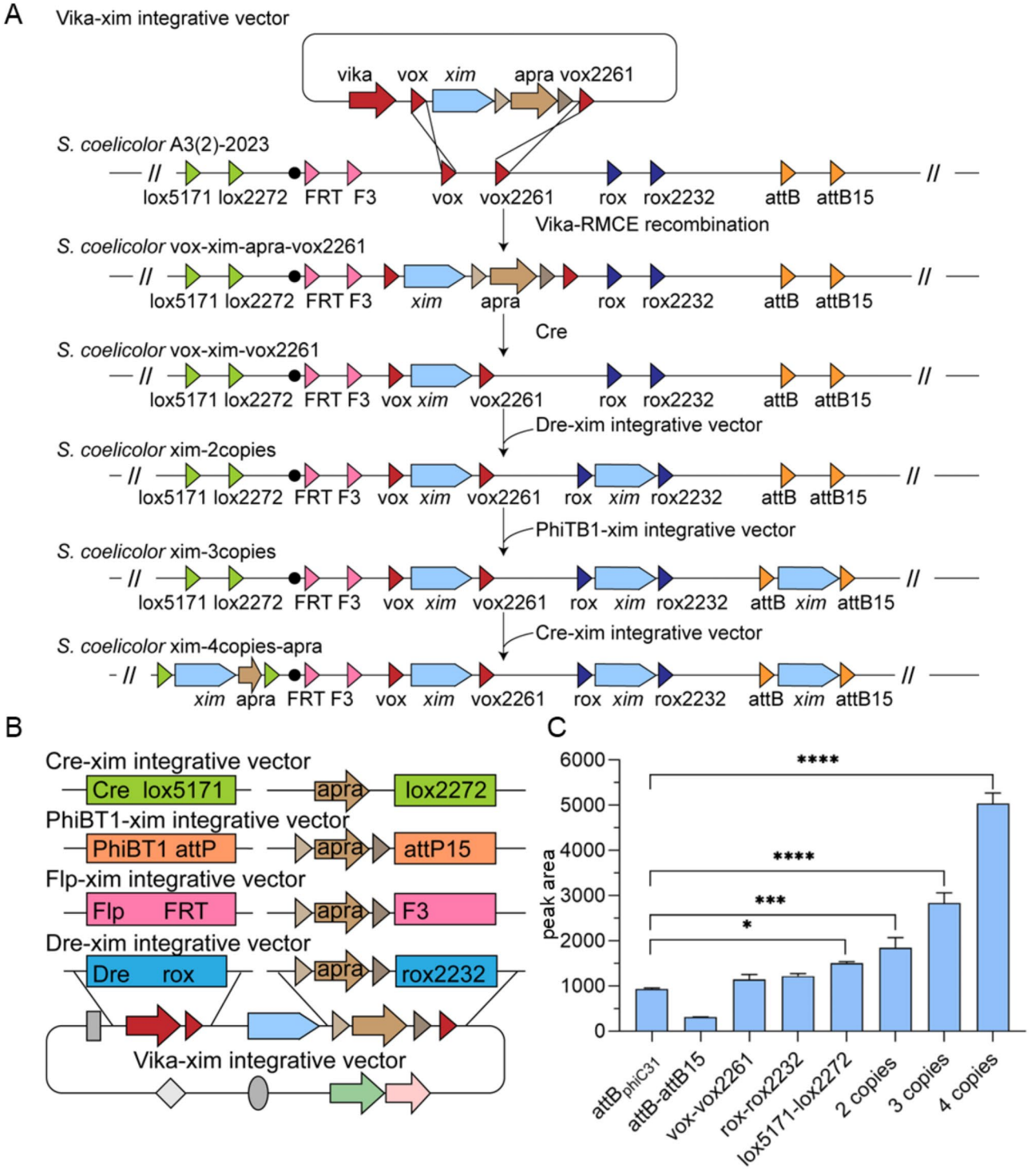

Fig. 4 Establishment of RMCE systems mediated by different recombinases in *S. coelicolor* A3(2)-2023. (**A**) An illustration of multicopy integration of the *xim* BGC into *S. coelicolor* A3(2)-2023 chromosome by RMCE recombination. Firstly, the donor strain *E. coli* GB05-recET-tra-αβγ containing the Vika integrative vector is conjugated with *S. coelicolor* A3(2)-2023, resulting in *xim* BGC integration into the vox-vox2261 site of A3(2)-2023 by Vika. Then, the apramycin resistance gene (apra) flanked by *lox71* and *lox66* is excised by Cre, resulting in a marker-free strain containing one copy of the BGC. Next, Dre, PhiBT1, and Cre integrative vectors are applied sequentially to complete insertion of multiple copies of the BGC via a similar method. (**B**) Design of the five integrative vectors containing the *xim* BGC. Each integrative vector contains an integrase gene and corresponding sites. The Vika-, Dre-, Flp-, and PhiBT1-based integrative vectors contain the apramycin resistance marker gene flanked by *lox71*and *lox66* sites. The Cre-based integrative vector contains only the apramycin resistance gene. The small brown arrows indicate *lox71* and *lox66*. (**C**) Comparison of the production of xiamenmycin in *S. coelicolor* strains harboring one or multiple copies of the *xim* BGC. Strain *S. coelicolor* xim-attB$_{phiC31}$ (attB$_{phiC31}$) is a control. Error bars indicate SD; $n = 3$; *$p < 0.05$; ***$p < 0.001$; ****$p < 0.0001$

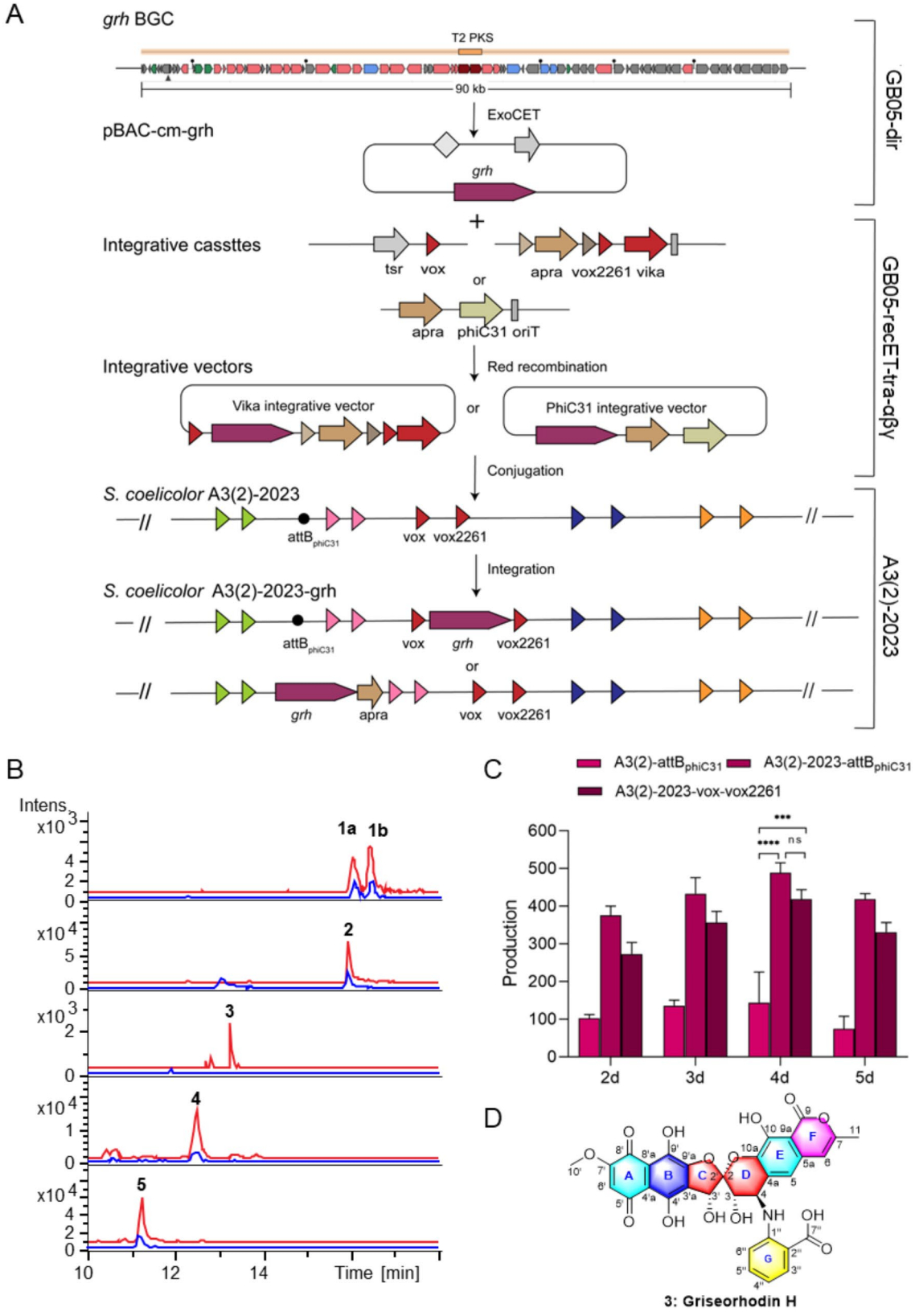

Fig. 5 (See legend on next page.)

(See figure on previous page.)

Fig. 5 Heterologous expression of the *grh* BGC from *Streptomyces* sp. LS-1 in the chassis strain *S. coelicolor* A3(2)-2023. (**A**) An illustration of the integration of the *grh* BGC into the chassis strain *S. coelicolor* A3(2)-2023. Firstly, the *Streptomyces* sp. LS-1 genome was analyzed by antiSMASH, and the 90 kb BGC *grh* was cloned into a pBAC vector by ExoCET. Secondly, Vika-based RMCE cassettes or the oriT-phiC31-apra cassette was inserted into pBAC-cm-grh by Red recombination in *E. coli* GB05-recET-tra-αβγ. Finally, BGC *grh* was integrated into the chromosome of the chassis strain and expressed. (**B**) Base peak chromatogram (BPC) analysis of fermentation extracts from *S. coelicolor* A3(2)-2023-grh-attB$_{phiC31}$ (red) and *S. coelicolor* A3(2)-grh-attB$_{phiC31}$ (blue): compound **1a/1b** (BPC 919.22 + all MS), compound **2** (BPC 475.09 + all MS), compound **3** (BPC 6 46.11 + all MS), compound **4** (BPC 511.08 + all MS), and compound **5** (BPC 527.07 + all MS). (**C**) Production of compound **2** at four time-points in *S. coelicolor* A3(2)-grh-attB$_{phiC31}$ (A3(2)-attB$_{phiC31}$), *S. coelicolor* A3(2)-2023-grh-attB$_{phiC31}$ (A3(2)-2023-attB$_{phiC31}$), and *S. coelicolor* A3(2)-2023-vox-grh-vox2261 (A3(2)-2023-vox-vox2261). (**D**) Chemical structure of compound **3**. Error bars indicate SD; $n = 3$; ns, $p > 0.05$; ***$p < 0.001$; ****$p < 0.0001$

the yield, such as overexpressing positive regulatory factors or deleting negative regulatory factors.

Large-scale fermentation of strain *S. coelicolor* A3(2)-2023-grh-attB$_{phiC31}$ containing the *grh* BGC was performed to enable further product separation and purification. Compounds **1**–**5** were successfully isolated and identified (Fig. 5B and Fig. S10). Compounds **1a** and **1b** are the known compounds griseorhodin D1 and griseorhodin D2; however, ^{13}C NMR data, such as for C-1, C-21, C-24, and C-25, had not been fully determined [43]. Therefore, we conducted additional 1D NMR data analysis for compounds **1a**/**1b** (Table S7). Compound **2** was identified as the known compound KS-619-1 [43], and HPLC analysis also verified that both compounds **1a** and **1b** were slowly converted to compound **2**. Compounds **4** and **5** were identified as the known compounds griseorhodin G and griseorhodin C, respectively. Compound **3**, a new compound, was obtained as a red powder and was named griseorhodin H (Fig. 5D). Griseorhodin H was not discovered in the crude extract of the *S. coelicolor* A3(2) strain containing the *grh* BGC (Fig. 5B). The observed metabolic divergence arises from the metabolic background of the chassis *S. coelicolor* A3(2)-2023, which lacks endogenous *red* and *act* BGCs. This deletion eliminates resource competition between native and heterologous pathways, enhancing metabolic flux toward the heterologously expressed *grh* BGC. By contrast, the A3(2)-2023 chassis elevates compound **3** production to detectable levels. The molecular formula of griseorhodin H was determined to be $C_{32}H_{23}NO_{14}$ by electrospray ionization–high-resolution mass spectrometry (ESI-HRMS) at *m/z* 644.1049 $[M-H]^-$. The planar structure, relative configuration, and absolute configuration of compound 3 were elucidated by extensive spectroscopic analyses (*SI Appendix*, Results and Table S8). These findings demonstrated that the chassis *S. coelicolor* A3(2)-2023 has superior potential for NP discovery and yield improvement compared with *S. coelicolor* A3(2). The Micro-HEP system developed in this study will provide an efficient platform for genome mining of novel NPs and enhancing production of important microbial drugs.

Discussion

In this study, *E. coli* engineered strains that would be capable of both modification and conjugative transfer of BGCs were constructed by integrating the dual function recombineering and transfer element tra-P$_{Rha}$-redαβγ into their chromosomes. The application of the bifunctional strains *E. coli* GB05-recETtra-αβγ and DH5G-Gtra-αβγ reduces electroporation steps and saves the time involved in DNA modification and transfer. Each of these strains has its own advantages with the former showing the highest efficiency of conjugation transfer and the latter showing a high recombination efficiency and generating the highest-quality plasmid preparation due to the high biomass of this strain. Because conjugation transfer efficiency decreases with increasing plasmid size, GB05-recETtra-αβγ would be more suitable for transferring large BGCs, whereas with small plasmids, DH5G-Gtra-αβγ would be recommended due to its high recombination efficiency for facilitating the modification of BGCs. While S17-1 derivative is widely recognized for its high conjugation efficiency (Fig. 2A) and stability of repetitive DNA (Fig. 2D), their utility is constrained by low electroporation efficiency for large plasmids (> 100 kb) (Fig. 2B). This limitation hinders their application in multi-step genetic manipulations (Gibson assembly or DNA editing), which are critical for modifying complex BGCs. Our bifunctional strain (both modify and transfer DNA) streamlines the workflow by avoiding intermediate strain switching. Additionally, *gyrA*, *dcm*, *dam*, *recA* and Mu on the *E. coli* chromosomes were modified by Redαβγ recombination combined with counterselection, and no additional resistance genes were added to the chromosomes of the engineered strains compared with the commonly used *E. coli* ET12567 (pUZ8002). Our strains conducive to the use of resistance genes for subsequent genetic manipulation and conjugation-mediated multiplex plasmid transformation [17].

In addition, in terms of the stability of plasmids containing repetitive sequences, the engineered strains performed better than *E. coli* ET12567 did, which will facilitate the cloning and modification of large BGCs containing large repetitive sequences (Table S9). Ensuring the stability of BGCs in *E. coli* without unanticipated intramolecular recombination is essential for the successful expression of BGCs [18]. Knockout of the *dam*

gene can reduce the stability of repetitive sequences in *E. coli* due to a Dam methylation-dependent deletion mechanism that causes DNA rearrangements [44]; loss of the *dam* gene can impede DNA repair in the presence of a methylated DNA strand, thereby leading to the rearrangements of the repeated sequences. To further improve the stability of our engineered strains derived from *E. coli* GB2005 and DH5G, we attempted inducing *dam* gene expression using arabinose or tryptophan-induced promoters. However, the results were not ideal. Plasmids were still methylated due to the leaky expression of *dam*. Therefore, further investigation is required to explore other genes or systems in *E. coli* that may contribute to maintaining stable plasmid replication.

PhiC31 integrase-mediated site-specific recombination has been extensively utilized for the stable chromosomal integration of target BGCs in *Streptomyces* [7]; however, in this study, RMCE method was used to integrate the target BGCs. Unlike PhiC31 integrase-mediated site-specific recombination, which integrates whole plasmids into chromosomes [45], RMCE systems use box exchange to integrate BGCs, which avoids the insertion of unnecessary sequences (plasmid replicons, recombinase genes, etc.) (Fig. 4A), thereby minimizing potential disruptions. The result of RMCE integration is similar to that of double-exchange recombination. And, RMCE does not require long homologous arms. Moreover, RMCE-mediated integration of BGCs using the recombinases Vika, Dre, and Cre expands the application of the tyrosine family of recombinases in *Streptomyces*. Vika has not previously been used in *Streptomyces*, and although the Dre and Cre recombinases have been used for DNA deletions in *Streptomyces* [46], no one has used them to complete the integration of BGCs in *Streptomyces* to our knowledge. Unfortunately, we were unable to establish Flp-mediated RMCE recombination in *S. coelicolor* A3(2)-2023. Due to a lack of successful Flp integrative vector under the promoter P_{ermE*} in *E. coli*, we suspected that using the promoter P_{ermE*} to control the Flp recombinase gene led to high Flp recombinase activity that resulted in the recombination of the FRT and F3 sites, so we then selected the weaker promoter $P_{sco1854}$ [47] for expression of the Flp recombinase and successfully obtained the correct integrative vector. However, in *Streptomyces*, expression of Flp under $P_{sco1854}$ control failed to result in complete RMCE recombination. Thus, to establish a Flp-mediated RMCE system, it will be necessary to explore other constitutive or inducible promoters for controlling Flp expression.

It has been reported that multiple $attB_{phiC31}$ sites were inserted into the *Streptomyces* chromosome as integration sites for multi-copy BGCs [22, 24] and the production of NP can be increased through increasing the number of copies of the target BGC. Increasing the copy number of BGC is one of the important methods to increase yield. Using our chassis strain *S. coelicolor* A3(2)-2023, two to four copies of the *xim* BGC was integrated into the chromosome and expression of xiamenmycin was increased with increased copy number. In addition, the multiple RMCE sites also will offer other strategies to increase production of NPs. It should be noted that having multiple RMCE sites not only allows for the insertion of more than one copy of a target BGC but also the addition of other genes such as regulatory genes or modified genes of the BGC since RMCE sites are recognized by different integrases and do not cross-recombine with each other. Therefore, this RMCE system can be used to overexpress BGCs to increase NP yield.

High-yield production of targeted compounds in an ideal chassis strain is a good approach for identifying complex or unstable structures. In this study, the 90 kb *grh* BGC from *Streptomyces sp*. LS-1 was heterologously expressed using our Micro-HEP system. We rapidly obtained large amounts of these compounds by expression of the *grh* BGC, enabling the full structural elucidation of these compounds by NMR and identing a new compound griseorhodin H. Our findings demonstrate that heterologous expression of BGCs using our Micro-HEP system can play a valuable role in the discovery of new NPs as well as provide high yields that allow further biochemical characterization of the products.

Conclusion

The Micro-HEP system based on engineered strain *E. coli* and chassis strain *S. coelicolor* enables the genetic modification, transfer, integration, and expression of biosynthesis gene clusters (BGCs) for natural products (NPs). The modular RMCE cassettes provide the transfer origin site oriT, integrases (Vika, Dre, Cre, and PhiBT1), and integrase-recognized RMCE sites for BGC transfer and chromosome integration. The engineered strain *E. coli* with inserted recombineering and conjugative transfer element tra-P_{Rha}-redαβγ on the chromosome, that can achieve modification and transfer of BGCs. The chassis strain *S. coelicolor* A3(2)-2023 contains multiple introduced RMCE sites and deletions of multiple endogenous BGCs, thereby facilitating the insertion of multiple copies of NP BGCs or their regulatory factors and reducing competition for precursors and energy. Heterologous expression of NP BGCs using our Micro-HEP system can not only facilitate the study of complex BGCs and improve the yield of target compounds, but also create novel synthetic pathways for the production of new active compounds with diverse structures.

Abbreviations

NPs	natural products
BGCs	biosynthetic gene clusters
RMCE	recombinase-mediated cassette exchange

RTSs	recombinase target sites
HPLC-MS	high-performance liquid chromatography–mass spectrometry

Supplementary Information

The online version contains supplementary material available at https://doi.org/10.1186/s12934-025-02722-z.

Supplementary Material 1

Acknowledgements
The authors thank Jingyao Qu, Jing Zhu, Zhifeng Li, and Guannan Lin from the State Key Laboratory of Microbial Technology of Shandong University for help and guidance in LC-MS.

Author contributions
J.F., R.L., G.L., and X.W. designed research; X.W., P.L., Q.S., X.F., S. X., Q.Z., Y.L., C.R., D.Y. and Q.D. performed research; X.W., P.L., Y.Z., R.L., and G.L. analyzed data; L.H., J.F. and R.L. supervised the study; and X.W., G.L., J.F., and R.L. wrote the paper. All authors reviewed the manuscript.

Funding
This work was supported by National Key Research & Development Program of China (2018YFA0900400 to J. F.), National Natural Science Foundation of China (32161133013, 32170038 to Y.Z.); the Taishan Scholar Program of Shandong Province (to J.F., R.L. and L.H.); the Shandong Provincial Natural Science Foundation of China (ZR2021ZD39 to J. F., ZR2020MC015 to R.J., ZR2023MC119 to G. L.); and the State Key Laboratory of Microbial Technology Open Projects Fund (Project NO. M2023-15 to J. F. and G. L.).

Data availability
No datasets were generated or analysed during the current study.

Declarations

Competing interests
The authors declare no competing interests.

Appendix A. Supporting information
Appendix (PDF)

Author details
[1]State Key Laboratory of Microbial Technology, Shandong University, Qingdao 266237, China
[2]Department of Natural Medicinal Chemistry and Pharmacognosy, School of Pharmacy, Qingdao University, Qingdao 266071, China

Received: 14 October 2024 / Accepted: 15 April 2025
Published online: 14 May 2025

References

1. Wang M, Li H, Li J, Zhang W, Zhang J: *Streptomyces* strains and their metabolites for biocontrol of phytopathogens in agriculture. *J Agric Food Chem* 2024, 72:2077–2088.
2. Selim MSM, Abdelhamid SA, Mohamed SS: Secondary metabolites and biodiversity of actinomycetes. *J Genet Eng Biotechnol* 2021, 19:72.
3. Lee N, Hwang S, Kim J, Cho S, Palsson B, Cho B K: Mini review: Genome mining approaches for the identification of secondary metabolite biosynthetic gene clusters in *Streptomyces*. *Comput Struct Biotechnol J* 2020, 18:1548–1556.
4. Kang H-S, Kim E-S: Recent advances in heterologous expression of natural product biosynthetic gene clusters in *Streptomyces* hosts. *Curr Opin Biotech* 2021, 69:118–127.
5. Nepal KK, Wang G: *Streptomycetes*: Surrogate hosts for the genetic manipulation of biosynthetic gene clusters and production of natural products. *BiotechnolAdv* 2019, 37:1–20.
6. Li Y, Xu Z, Chen P, Zuo C, Chen L, Yan W, Jiao R, Ye Y: Genome mining and heterologous expression guided the discovery of antimicrobial naphthocyclinones from *Streptomyces eurocidicus* CGMCC 4.1086. *J Agric Food Chem* 2023, 71:2914–2923.
7. Liu R, Deng Z, Liu T: *Streptomyces* species: Ideal chassis for natural product discovery and overproduction. *Metab Eng* 2018, 50:74–84.
8. Medema MH, Blin K, Cimermancic P, de Jager V, Zakrzewski P, Fischbach MA, Weber T, Takano E, Breitling R: antiSMASH: rapid identification, annotation and analysis of secondary metabolite biosynthesis gene clusters in bacterial and fungal genome sequences. *Nucleic Acids Res* 2011, 39:W339-346.
9. Wang H, Li Z, Jia R, Yin J, Li A, Xia L, Yin Y, Müller R, Fu J, Stewart AF, Zhang Y: ExoCET: exonuclease in vitro assembly combined with RecET recombination for highly efficient direct DNA cloning from complex genomes. *Nucleic Acids Res* 2018, 46:2697.
10. Li R, Li A, Zhang Y, Fu J: The emerging role of recombineering in microbiology. *Eng Microbiol* 2023, 3:100097.
11. Abbasi MN, Fu J, Bian X, Wang H, Zhang Y, Li A: Recombineering for genetic engineering of natural product biosynthetic pathways. *Trends Biotechnol* 2020, 38:715–728.
12. Virolle C, Goldlust K, Djermoun S, Bigot S, Lesterlin C: Plasmid transfer by conjugation in gram-negative bacteria: from the cellular to the community level. *Genes (Basel)* 2020, 11:1239.
13. Silbert J, Lorenzo Vd, Aparicio T: Refactoring the conjugation machinery of promiscuous plasmid RP4 into a device for conversion of gram-negative isolates to Hfr strains. *ACS Synth Biol.* 2021, 10:690–697.
14. Zatyka M, Jagura-Burdzy G, Thomas CM: Regulation of transfer genes of promiscuous IncP alpha plasmid RK2: repression of Tra1 region transcription both by relaxosome proteins and by the Tra2 regulator TrbA. *Microbiology(Reading)* 1994, 140 (Pt 11):2981–2990.
15. MacNeil DJ, Gewain KM, Ruby CL, Dezeny G, Gibbons PH, MacNeil T: Analysis of *Streptomyces avermitilis* genes required for avermectin biosynthesis utilizing a novel integration vector. *Gene* 1992, 111:61–68.
16. Flett F, Mersinias V, Smith CP: High efficiency intergeneric conjugal transfer of plasmid DNA from *Escherichia coli* to methyl DNA-restricting *Streptomycetes*. FEMS *Microbiol Lett.* 1997, 155:223–229.
17. Ko B, D'Alessandro J, Douangkeomany L, Stumpf S, deButts A, Blodgett J: Construction of a new integrating vector from actinophage ϕOZJ and its use in multiplex *Streptomyces* transformation. *J Ind Microbiol Biot* 2020, 47:73–81.
18. Tan G Y, Deng K, Liu X, Tao H, Chang Y, Chen J, Chen K, Sheng Z, Deng Z, Liu T: Heterologous biosynthesis of Spinosad: An omics-guided large polyketide synthase gene cluster reconstitution in *Streptomyces*. *ACS Synth Biol* 2017, 6:995–1005.
19. Myronovskyi M, Luzhetskyy A: Heterologous production of small molecules in the optimized *Streptomyces* hosts. *Nat Prod Rep* 2019, 36:1281–1294.
20. McDaniel R, Ebert-Khosla S, Hopwood DA, Khosla C: Engineered biosynthesis of novel polyketides. *Science* 1993, 262:1546–1550.
21. Gomez-Escribano JP, Bibb MJ: Engineering *Streptomyces coelicolor* for heterologous expression of secondary metabolite gene clusters. *Microb Biotechnol.* 2011, 4:207–215.
22. Li L, Zheng G, Chen J, Ge M, Jiang W, Lu Y: Multiplexed site-specific genome engineering for overproducing bioactive secondary metabolites in actinomycetes. *Metab Eng* 2017, 40:80–92.
23. Myronovskyi M, Rosenkränzer B, Nadmid S, Pujic P, Normand P, Luzhetskyy A: Generation of a cluster-free *Streptomyces albus* chassis strains for improved heterologous expression of secondary metabolite clusters. *Metab Eng* 2018, 49:316–324.
24. Ahmed Y, Rebets Y, Estévez MR, Zapp J, Myronovskyi M, Luzhetskyy A: Engineering of *Streptomyces lividans* for heterologous expression of secondary metabolite gene clusters. *Microb Cell Fact* 2020, 19:5.
25. Aubry C, Pernodet JL, Lautru S: Modular and integrative vectors for synthetic biology applications in *Streptomyces* spp. *Appl Environ Microbiol* 2019, 85: e00485–19.
26. Sevillano L, Díaz M, Santamaría RI: Development of an antibiotic marker-free platform for heterologous protein production in *Streptomyces*. *Microb Cell Fact* 2017, 16:164.
27. Karimova M, Abi-Ghanem J, Berger N, Surendranath V, Pisabarro MT, Buchholz F: Vika/vox, a novel efficient and specific Cre/loxP-like site-specific recombination system. *Nucleic Acids Res* 2013, 41:e37.
28. He L, Li Y, Li Y, Pu W, Huang X, Tian X, Wang Y, Zhang H, Liu Q, Zhang L, et al: Enhancing the precision of genetic lineage tracing using dual recombinases. *Nat Med* 2017, 23:1488–1498.
29. Araki K, Yamamura K-i: Genetic manipulations using Cre and mutant loxP Sites. In *Controlled Genetic Manipulations.* Edited by Morozov A. Totowa, NJ: Humana Press; 2012: 29–45.

30. Roux I, Chooi YH: Cre/lox-mediated chromosomal integration of biosynthetic gene clusters for heterologous expression in *Aspergillus nidulans*. *ACS Synth Biol* 2022, 11:1186–1195.
31. Srirangan K, Loignon M, Durocher Y: The use of site-specific recombination and cassette exchange technologies for monoclonal antibody production in Chinese Hamster ovary cells: retrospective analysis and future directions. *Crit Rev Biotechnol* 2020, 40:833–851.
32. Yuzawa S, Mirsiaghi M, Jocic R, Fujii T, Masson F, Benites VT, Baidoo EEK, Sundstrom E, Tanjore D, Pray TR, et al: Short-chain ketone production by engineered polyketide synthases in *Streptomyces albus*. *Nature Commun* 2018, 9:4569.
33. Kieser T, Bibb MJ, Buttner MJ, Chater KF, Hopwood DA, Charter K, Bib MJ, Bipp M, Keiser T, Butner M: Practical *Streptomyces* Genetics. John Innes Foundation 2000.
34. Simon R, Priefer U, Pühler A: A broad host range mobilization system for in vivo genetic engineering: transposon mutagenesis in gram negative bacteria. Bio/Technology 1983, 1:784–791.
35. Wang X, Zhou H, Chen H, Jing X, Zheng W, Li R, Sun T, Liu J, Fu J, Huo L, et al: Discovery of recombinases enables genome mining of cryptic biosynthetic gene clusters in Burkholderiales species. *Proc Natl Acad Sci U S A* 2018, 115:E4255-E4263.
36. Tian Y, Li D, Wang K, Wei B, Zhang J, Li J: An efficient method for targeted cloning of large DNA fragments from *Streptomyces*. *Appl Microbiol Biotechnol* 2023, 107:5749–5760.
37. Bryant JA, Sellars LE, Busby SJW, Lee DJ: Chromosome position effects on gene expression in *Escherichia coli* K-12. *Nucleic Acids Res* 2014, 42:11383–11392.
38. Ferrières L, Hémery G, Nham T, Guérout AM, Mazel D, Beloin C, Ghigo JM: Silent mischief: bacteriophage Mu insertions contaminate products of *Escherichia coli* random mutagenesis performed using suicidal transposon delivery plasmids mobilized by broad-host-range RP4 conjugative machinery. *J Bacteriol* 2010, 192:6418–6427.
39. Wang H, Bian X, Xia L, Ding X, Müller R, Zhang Y, Fu J, Stewart AF: Improved seamless mutagenesis by recombineering using *ccdB* for counterselection. *Nucleic Acids Res* 2013, 42:e37.
40. Cunha MV, Yang Y, Fu L, Zhang J, Hu L, Xu M, Xu J: Characterization of the xiamenmycin biosynthesis gene cluster in *Streptomyces xiamenensis* 318. *PLoS ONE* 2014, 9:e99537.
41. Toplak M, Saleem-Batcha R, Piel J, Teufel R: Catalytic control of spiroketal formation in rubromycin polyketide biosynthesis. *Angew Chem Int Ed Engl* 2021, 60:26960–26970.
42. Lin P, Li X, Xin Y, Li H, Li G, Lou H: Isolation, biosynthesis, and biological activity of rubromycins derived from actinomycetes. *Eng Microbiol* 2022, 2:100039.
43. Lin Z, Zachariah MM, Marett L, Hughen RW, Teichert RW, Concepcion GP, Haygood MG, Olivera BM, Light AR, Schmidt EW: Griseorhodins D–F, neuroactive intermediates and end products of post-PKS tailoring modification in griseorhodin biosynthesis. *J Nat Prod* 2014, 77:1224–1230.
44. Troester H, Bub S, Hunziker A, Trendelenburg MF: Stability of DNA repeats in *Escherichia coli dam* mutant strains indicates a Dam methylation-dependent DNA deletion process. *Gene* 2000, 258:95–108.
45. Siegl T, Luzhetskyy A: Actinomycetes genome engineering approaches. *Antonie van Leeuwenhoek* 2012, 102:503–516.
46. Bu QT, Yu P, Wang J, Li ZY, Chen XA, Mao XM, Li Y Q: Rational construction of genome-reduced and high-efficient industrial *Streptomyces* chassis based on multiple comparative genomic approaches. *Microb Cell Fact* 2019, 18:16.
47. Li S, Wang J, Li X, Yin S, Wang W, Yang K: Genome-wide identification and evaluation of constitutive promoters in streptomycetes. *Microb Cell Fact* 2015, 14:172.

Publisher's note